

Advances in spaceborne hyperspectral imaging systems

K. Ajay Kumar*, Nitesh Thapa and Saji A. Kuriakose

Sensor Development Area, Space Applications Centre, ISRO, Ahmedabad 380 015, India

Here we discuss hyperspectral imaging techniques and present an overview of a number of systems that have been developed by various space agencies. We also present the evolution of these systems and the progress made by the Indian space programme in this field.

Keywords: Hyperspectral instruments, imaging, remote sensing, spectral bands, spectrometry.

Introduction

REMOTE sensing is the ability to obtain information without making physical contact with the object to be studied. Depending upon the number of spectral bands, sensors are classified as panchromatic (single band), multi-spectral (more than one band) and hyperspectral (a large number of contiguous bands). The spectral information content varies in these three classes of sensors and they have their relative merits. They find usage in different applications and each has a niche area of use.

Hyperspectral imaging sensors (HySI) combine two sensing techniques familiar to the scientific community – imaging and spectrometry. These sensors capture the two-dimensional spatial distribution of the reflected or emitted electromagnetic radiation along with the variation in signal with wavelength¹. Thus, it forms a data cube having two spatial dimensions and a spectral dimension as shown in Figure 1.

Scanning techniques

The primary design challenge is to produce a hyperspectral data cube, which is three-dimensional data, with two spatial dimensions and one spectral dimension, while focal plane arrays (FPA) image in two dimensions. Thus, it is not possible to capture complete 3D information of a scene at an instant using a 2D sensor. Therefore, a method is required to capture the additional dimension. This is often carried out using time as the third dimension¹. Temporal scanning is carried out in either spectral or spatial direction. Some devices disperse the incoming

field into different wavelengths which are then imaged by the detector. Spatial scanning is carried out for such instruments by moving the platform or using a scan mirror along the direction of dispersion (known as push-broom scanning). Some instruments acquire the spatial 2D information at every instant and carry out the spectral scanning using Fourier transformation techniques or using tuneable filters. This method requires that there is no relative motion between the platform and the scene until the desired spectrum is scanned completely. Sensors based on linearly variable filters (LVF) acquire information in both spectral and spatial domain simultaneously to form a 2D array and generate a 3D cube by push-broom scanning.

Hyperspectral imaging sensor design

A HySI system consists of a fore optics for the collection of the scene radiance, a device for spectral separation, a focusing optics and a focal plane array for detection. In general, three types of spectral separation devices/subsystems are usually used: (i) Dispersive spectrometers; (ii) Fourier transform interferometers, and (iii) Narrow-band adaptive filters.

Dispersive spectrometer

Prisms or gratings are used for spectral dispersion. Typically a collimated beam of light is incident on a prism,

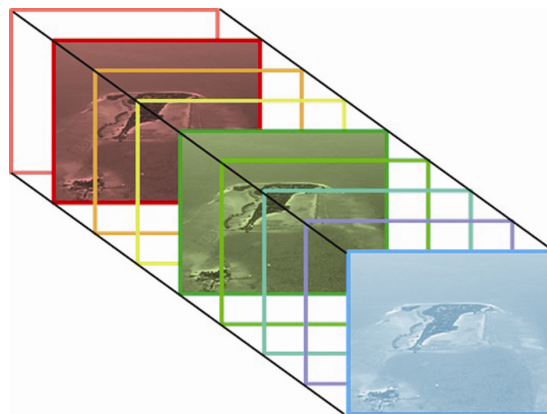


Figure 1. Representation of HySI data cube showing a two-dimensional scene with spectral information.

*For correspondence. (e-mail: ajaykumar@sac.isro.gov.in)

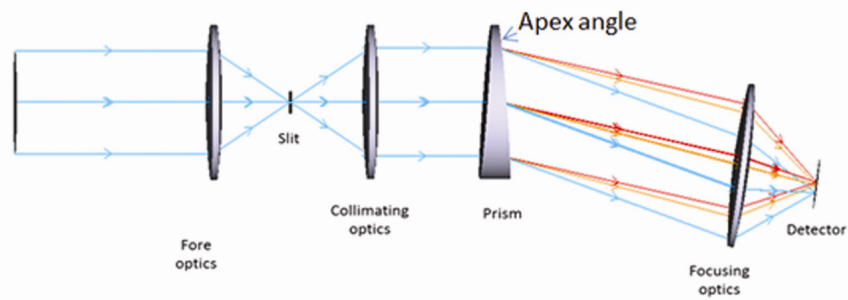


Figure 2. Schematic optical configuration of a prism-based spectrometer.

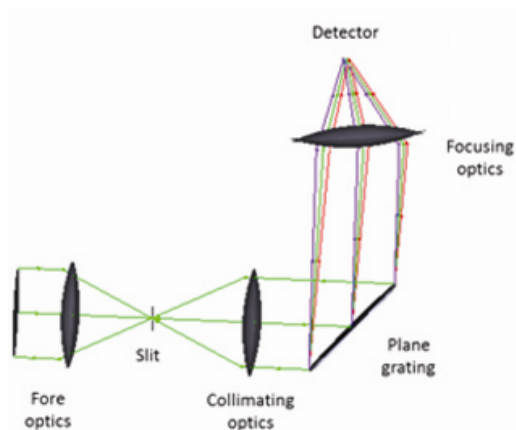


Figure 3. Schematic optical configuration of a reflective grating-based spectrometer.

which results in angular dispersion of the incident light into different wavelength components. This configuration is shown in Figure 2. The thickness of the glass prism as well as its wedge shape contribute to a large amount of aberrations in such instruments. To minimize aberrations over the field, imaging spectrometers sometimes employ a combination of prisms with curved surfaces, wavefront correction optics and double-pass spectrometer arrangements. The Littrow arrangement is a common design form that employs a parabolic mirror². An advanced double aplanatic prism spectrometer design approach based on spherical prism surfaces, achieves low aberrations at low f-number, larger field of view and larger spectral range³.

Plane diffraction grating-based systems can vary the spectral dispersion by modifying grating design. Figure 3 shows a typical reflective plane grating-based spectrometer. Plane-grating and prism-based systems require collimated light beams for generating a plane wavefront and subsequent focusing optics for converting dispersed plane wavefront back into spherical wavefront. Blazed grating can be used to increase the grating efficiency for a particular diffraction order and wavelength. Grating-based systems suffer from multi-order diffraction which is generally addressed by employing order-sorting filters.

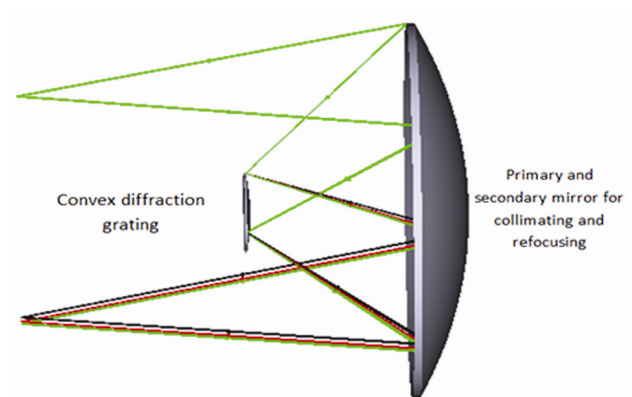


Figure 4. Schematic optical configuration of an Offner-based spectrometer.

Offner spectrometer is an adaptation of classical Offner imaging relay in the form of a spectrometer (Figure 4). It is simpler as it does not require conversion of spherical wavefront to plane wavefront and vice versa. Concentric imaging relay has excellent image quality and is compact and achromatic as it comprises of only mirrors; however, it provides comparatively low spectral resolution. This requires a convex grating, manufacturing of which is more difficult and much more costly than a plane grating. Due to asymmetry caused by the diffraction grating, it usually suffers with spectral-spatial distortions (keystone and smile). With advancement in fabrication techniques and realization of volume phase holographic (VPH) gratings, various advanced designs like half-Offner, spherical transmission grating spectrometer (STGS), etc. are now available which are superior to classical Offner spectrometers⁴.

Another concentric imaging design is the Dyson variety based on a spherical mirror, a thick Dyson lens (hemispherical lens) and optional corrector optics (Figure 5). The curved lens surface and mirror are concentric and image plane is located near the flat surface of the lens. This is comparatively compact compared to the prism and grating spectrometers. The Dyson design is adapted as a spectrometer by replacing the spherical mirror by a grating surface on the concave surface. To minimize the

spherical and chromatic aberrations, a meniscus corrector lens is frequently used. The Dyson spectrometer is more sensitive to fabrication tolerance and misalignment of components compared to the prism and grating spectrometers⁵.

Fourier transform interferometers

Fourier transform interferometers include Michelson interferometer or Sagnac interferometer. The common principle of these two interferometers is splitting of the radiation from a source into two beams, introducing a controlled phase shift, and recombining them generating interference. The intensity of the light is modulated by the path difference of the two beams. The amplitude of the signal is sampled at an appropriate sample rate during the acquisition, and a Fourier transform converts the amplitude modulated signal into a frequency spectrum. It is also called Fourier transform infrared (FTIR) spectrometer because it has been used traditionally in MWIR and LWIR spectral regions. It has high spectral resolution as it is only limited by mechanical parameters and not the characteristics of the dispersing component. It has finer spectral resolution, comparatively higher optical throughput and better spectral accuracy. FTS approach, both temporal and spatial, provides better performance when the system is noise-limited. Therefore, the spatial FTS can provide a means for achieving decent radiometric performance using low-cost FPAs⁶.

Linear variable filters

A LVF is a band-pass filter in which the thickness of the filter coating varies linearly along its length so that the spectral content transmitted through it varies in that direction resulting in principle in an unlimited number of different filters (Figure 4). Hence, the number of separate spectral channels depends solely on the number of elements in the detector array. It is also called a wedge filter. Telecentric optics is required for systems having

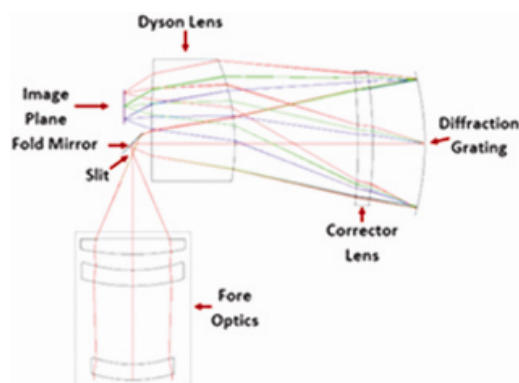


Figure 5. Optical schematic of a Dyson-based spectrometer.

large field of view as the transmission characteristic of LVF varies significantly with the angle of incidence. It has moderate spectral resolution of a few tens of nanometres. This spectrometer does not have inherent registration of all spectral bands.

Acousto-optic tuneable filters

An acousto-optic tunable filter (AOTF) is a pass-band transmission filter, which exploits the acousto-optic interaction inside an anisotropic medium. Crystal (generally quartz) is placed on the piezoelectric transducer, which allows the crystal to vibrate at certain frequency (generally radio frequency) changing the refractive index of the glass causing it to act like a Bragg grating. Incoming light scatters the resulting periodic index modulation and interference occurs similar to Bragg diffraction. Frequency of the excitation source is varied to change the period of the grating formed and thus select the required transmission wavelength. The advantages of the AOTF are the short response time (typically microseconds) and the consequent fast spectral band selection, absence of moving parts, compactness and a wide angular aperture. But the AOTF cannot capture simultaneous spectral information and for large number of bands the time taken for measurement also increases. It also has low optical throughput, relatively complex optical design and very high power requirement. These limitations inhibit the use of the approach for airborne or space-based terrestrial imaging applications, especially when fine spatial resolution is needed¹.

Tuned etalon

The Fabry–Perot etalon is the basis of tuned etalon spectral imagers. The etalon is the core element of the Fabry–Perot interferometer and is basically composed of two plane parallel partially reflecting surfaces with a precise spacing between them. A typical schematic of the etalon is shown in Figure 7. The etalon produces very narrow bands and filter characteristics like central wavelength and bandwidth can be tuned by varying the separation between the parallel surfaces or by electrically controlling the refractive index of the etalon material.

It has limitations like limited field of view owing to transmission characteristic dependency on angle of

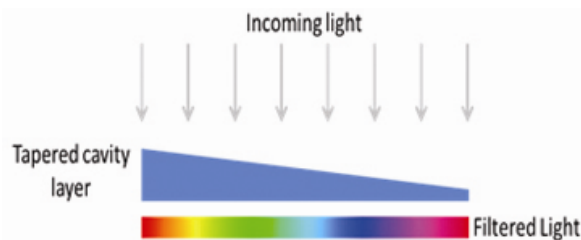


Figure 6. Typical schematic of LVF filter.

Table 1. Comparison of various techniques used in spectrometers

Property	Grating	Prism	FT spectrometer	LV filter
Spectral resolution	High	Medium	Very high	Medium
Throughput	High	Medium	High	Medium
Spectral range	Broad	Narrow	Broad	Medium
Sensitivity to S/C motion	No	No	Yes	No
Moving parts	No	No	No/yes	No
Simultaneous acquisition	Yes	Yes	Yes	No
Stray light	Low	Low	High	High
Complexity	Low	Low	Very high	Very low
Distortion	Low/high*	High	Low	Medium
Compactness	Medium	Medium	Low	High

*Low for convex and concave grating, high for plane grating.

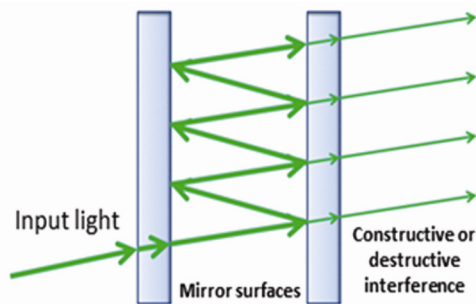


Figure 7. Typical schematic of etalon.

incidence and its sensitivity to temperature variation. Moreover, the operating wavelength range is limited compared to that of the other configurations.

Comparison

Table 1 provides a comparison between various techniques that have been employed by different instruments used for remote sensing applications. Techniques are selected based on requirements and constraints of the desired system.

HySI systems developed by various space agencies

The ultraviolet/visible imaging and spectrographic imaging (UVISI) consisted of nine instruments, of which five were spectrographic or hyperspectral imagers. It was for the first time that a hyperspectral spaceborne instrument was flown by the Department of Defence, USA, in April 1996. The objective of the mission was to collect data on celestial and atmospheric background to enable surveillance and target characterization. All five HySI systems were reflective off-axis parabolic mirror-based designs with a scanning mirror, selectable slit and filter, collimating mirror, dispersive grating and an intensified CCD

focal plane. It covered spectral range from 113 to 902 nm with resolution varying from 0.5 to 2.9 nm (ref. 7).

The Fourier transform hyperspectral imager was launched on MightySat II made by the US Air Force Research Laboratory in July 2000. It used a Sagnac-based interferogram, along with Fourier lens and cylindrical lens with an area array detector. It covered a spectral range of 475–1050 nm with a resolution of 1.7 nm at 450 nm (ref. 8).

The Hyperion was one of the hyperspectral instruments in Earth Observation Mission (EO-I), which was launched by NASA in 2000. It consisted of two convex grating based spectrometer with fore optics and focal plane array, covering both ‘visible and near infrared (VNIR 400–1000 nm)’ and ‘shortwave infrared (SWIR 900–2500 nm)’ with a spectral resolution of 10 nm in both spectral regions. For the SWIR instrument, a cooling system was incorporated to minimize the background⁹.

LEISA (linear etalon imaging spectral array) atmospheric corrector (LAC) provided atmospheric correction data for the enhanced thematic mapper (ETM) sensor on Landsat-7 and the advanced land imager (ALI) instrument on EO-I. It used wedge filter-based designs and operated in the spectral range 0.93–1.58 μm with 256 channels having spectral resolution better than 10 nm. The use of the wedged filter greatly simplifies the optical/mechanical design, so that the instrument is adaptable to a wide variety of platforms¹⁰.

The compact high resolution imaging spectrometer (CHRIS) was developed by ESA for the PROBA mini-satellite mission flown in 2001, and launched by ISRO. It used a prism along with Offner-based relay optics to increase the dispersion. The dispersion varied from 1.25 to 11 nm working in the wavelength range 400–1050 nm (ref. 11).

The SCIAMACHY (scanning imaging absorption spectrometer for atmospheric cartography) on-board ENVISAT was launched by ESA in 2002. It contained eight spectral channels, two in each of spectral regions (i.e. UV, VIS, NIR and SWIR) and used gratings for dispersion. In addition, it also used a prism for increased dispersion in the

UV channel. The dispersion varied from 0.22 to 1.48 nm working in the wavelength range 240–2380 nm (ref. 12).

The hyperspectral imager (HSI) of the HJ-1A mission which was launched by CAST (China) in 2008 used an interferometer, Fourier mirror, a calibration system, swing mirror and a detector array. It operated from 450 to 950 nm with an average spectral resolution of 5 nm (ref. 13).

The ARTEMIS (advanced responsive tactically effective military imaging spectrometer) was launched in TACSAT-3 Mission funded by US Army. It used an Offner grating along with two parabolic mirrors. It had a spectral resolution of 5 nm in the spectrum range covering 400 to 2500 nm (ref. 14).

Hyperspectral payloads developed by ISRO

Airborne imaging spectrometer (AIMS) was the first spectrometer developed by SAC-ISRO in 1996. It had 143 bands covering the spectral range from 454 to 888 nm with spectral resolution from 2.8 to 4.3 nm with SNR of about 400. The instrument utilized commercial optics for the fore optics, collimating and focusing optics. The dispersion was obtained with a plane grating. Figure 8 shows the AIMS instrument developed. This was used for aircraft flights intermittently from 1996 to 2013, when it was replaced by a newer instrument. The challenges in developing this instrument included the optical design, optical layout, optics system development, detector head assembly development, spectral characterization, performance optimization and measurement as well as design of the mechanical structure to survive the forces experienced during handling and aircraft flights.

The airborne hyperspectral imager (AHySI) was developed by SAC-ISRO in 2007. It is based on the wedge filter and covers the spectral range from 465 to 995 nm in 512 contiguous bands with spatial resolution of 15 nm. The wedge filter is placed in close proximity to the detector. Figure 9 shows the developed AHySI instrument. The wedge filter is placed such that spectral definition takes place in the along-track direction. Across-track

generates one dimension of spatial distribution and the other dimension is generated by push-broom scanning of the sensor. Full spectrum of the ground scene is obtained after it is traversed completely by the sensor by a long track movement. The challenges in the development of this sensor included the mechanical mount design of the very thin and fragile wedge filter, alignment of the filter, design and indigenous development of a telecentric lens assembly and finally the performance demonstration of the instrument.

The Indian mini satellite (IMS-1), was the first of ISRO's mini-satellites launched in 2008. The HySI wedge filter based instrument was first flown on this mission with a spectral resolution of 15 nm over the spectral range 450–950 nm. It was ISRO's first experience with the design and development of a spaceborne HySI payload. The system performed to expectations and is still operational. Figure 10 shows the photograph of HySI payload flown on IMS-1 (ref. 15).

The next wedge filter-based HySI instrument was designed to enable mineralogical mapping of the lunar crust in a large number of spectral channels. Along with HySI, ten other instruments were launched in Chandrayaan-1 in 2008. Design-wise it was similar to the spectrometer flown on-board IMS-1. It had a spectral range from 450



Figure 9. AHySI instrument.

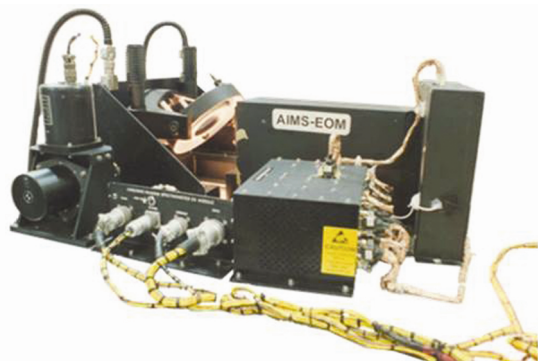


Figure 8. AIMS instrument.

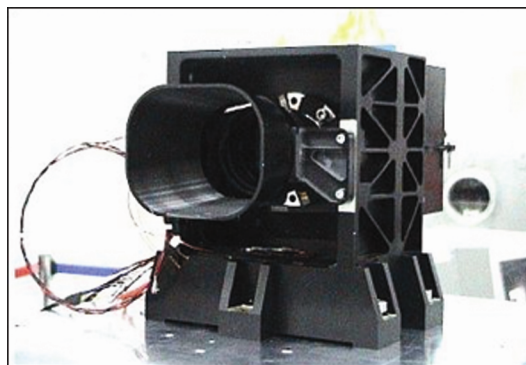


Figure 10. HySI instrument.

to 900 nm in 64 contiguous bands with a spectral resolution better than 15 nm and spatial resolution of 80 m. The collecting optics was a telecentric F/4 refractive optics designed and fabricated by ISRO. The spectrometer was designed with a wedge filter as the spectral selection element ensuring compactness and simplicity in implementation. An active pixel sensor (APS) area array detector with built-in digitizer mapped the spatial and spectral information. Payload is shown in Figure 11; its mass was 2.5 kg with dimensions of 275 mm × 255 mm × 205 mm (ref. 16).

After the success of HySI, an instrument for the study of airglow in the atmosphere was designed and developed. This instrument was flown on-board Youthsat in 2011 and was named Limb View HySI (LiVHySI). It was a wedge filter-based instrument operating from 450 to 950 nm with a spatial resolution of 4 km and a spectral resolution of 8 nm. LiVHySI was an improved version of the earlier developed HySI sent on the Chandrayan-1 mission. The spectral channels were increased from 64 to 512 and the radiometric performance was improved by replacing F/4 optics with F/2 and also optimizing detector operating conditions. The lens assembly was designed by ISRO and developed and qualified using Indian industry (Figure 12). A sensitivity of 50 Rayleigh has been achieved. The spectrum was sampled at 1 nm intervals. The objective of the mission was to perform airglow measurements and altitude profiles of neutral and ionized species of earth upper atmosphere (100–1100 km)¹⁷.

The thermal infrared imaging spectrometer (TIS) on-board the Mars Orbiter Mission (MOM) is a grating-based spectrometer with a spectral coverage range 7–13 μm with a spectral resolution of 58 nm. The TIS

instrument weighs 4 kg and consists of a spectrometer that features a typical infrared grating spectrometer design. The infrared radiation is focused on an entrance slit by a fore optics lens assembly. The slit is placed at the focus of a collimator so that collimated radiation is incident on a diffraction grating that acts as the dispersive element. A focus lens assembly focuses the dispersed radiation onto a detector. TIS uses a 120 × 160 element bolometer array detector. The TIS flown on-board MOM is shown in Figure 13. TIS measures the thermal emission and can be operated both during day and night. Temperature and emissivity are the two basic physical parameters estimated from thermal emission measurement. Many minerals and soil types have characteristic spectra in the TIR region and TIS can map surface composition and mineralogy of Mars.

ISRO is working on the development of geo-imaging satellite (GISAT), which is planned to be flown in 2017. One of the prime applications of this satellite is to generate hyperspectral imageries in VNIR and SWIR bands for spectral signatures/fingerprinting in agriculture, forestry, mineralogy, oceanography and other such remote sensing applications over the Indian region. It will cover spectral range from 0.4 to 1.0 μm and 0.9 to 2.5 μm



Figure 11. Chandrayaan-1 HySI.



Figure 12. LiVHySI instrument.

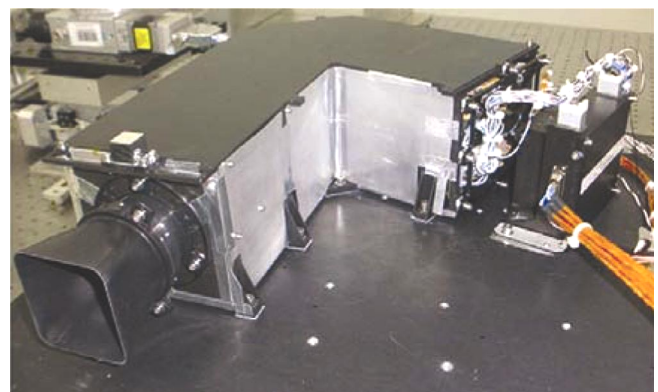


Figure 13. TIS instrument.

respectively, with about 200 contiguous bands having average spectral resolution of 10 nm in both the regions with a spatial resolution of 500 m from geostationary orbit. It will comprise of a main RC telescope with 700 mm aperture and the various channels will be separated using different fields for different wavelengths. Both the hyperspectral images (VNIR and SWIR) will be transmitted through their corresponding entrance slits and the spectral separation will be done using convex grating based Offner spectrometers.

Imaging infrared spectrometer (IIRS), the hyperspectral optical imaging instrument, will be flown on-board Chandrayaan-2 spacecraft. It will map the lunar surface with high spatial and spectral resolution supplementing the measurements carried out by instruments on-board Chandrayaan-1. The orbiter-based IIRS is an advanced version of the HySI spectrometer flown on-board Chandrayaan-1 and will carry out mineralogical investigations and identification of lunar silicate minerals. It will have a spatial resolution of 80 m and will cover a spectral range 0.8–5 μm with more than 200 contiguous bands having spectral resolution better than 20 nm. Convex grating-based single-Offner spectrometer with reflective fore optics (three mirror anastigmat) configuration is selected to cover a wide wavelength range. HgCdTe-based detector array is planned to be put at the focal plane of the spectrometer. The detector array with four-band monolithic filter strip (would serve dual purposes of order sorting and background flux reduction) is integrated in Dewar configuration and cooled to cryogenic temperature for operation using rotary Stirling cooler.

Conclusion

In this article we have briefly discussed hyperspectral instruments and the various configuration details and also some of the advanced systems that are being developed. We have also discussed the various instruments developed by space agencies worldwide. In addition, the hyperspectral instruments developed by ISRO and flown since the 1990s as well as those being developed have been presented.

1. Eismann, M. T., *Hyperspectral Remote Sensing*, SPIE Press, 2012, ISBN: 9780819487872.
2. Sidran, M., Stalzer, H. J. and Hauptmann, M. H., Drum dispersion equation for Littrow-type prism spectrometers. *Appl. Opt.*, 1966, **5**, 1133–1138.
3. Warren, D. W., Hackwell, J. A. and Gutierrez, D. J., Compact prism spectrographs based on aplanatic principles. *Opt. Eng.*, 1997, **36**, 1174–1182; doi:10.1117/1.601237.

4. O'Donoghue, D. and Christopher Clemens, J., Spherical grating spectrometers. In Proceedings of SPIE 9147, Ground-based and Airborne Instrumentation for Astronomy V, 914748, 8 July 2014; doi:10.1117/12.2055385.
5. Warren, D. W., Gutierrez, D. J., Hall, J. L. and Keim, E. R., Dyson spectrometers for infrared earth remote sensing. In Proceedings of SPIE 7082, Infrared Spaceborne Remote Sensing and Instrumentation XVI, 70820R, 3 September 2008; doi:10.1117/12.798419.
6. Wolfe, W. L., *Introduction to Imaging Spectrometers*, SPIE Press, Bellingham, WA, 1997; doi:10.1117/3.263530.
7. Heffernan, K. J., Heiss, J. E., Boldt, J. D., Darlington, E. H., Peacock, K., Harris, T. J. and Mayr, M. J., *The UVISI Instrument*, Johns Hopkins APL Technical Digest, vol. 17, no. 2, 1996, pp. 198–214.
8. Yarbrough, S. *et al.*, MightySat II.1 hyperspectral imager: summary of on-orbit performance. In Proceedings of SPIE 4480, Imaging Spectrometry VII, 186, 21 January 2002; doi:10.1117/12.453339.
9. Pearlman, J., Carman, S., Segal, C., Jarecke, P., Barry, P. and Browne, W., Overview of the Hyperion imaging spectrometer for the NASA EO-1 mission; http://eo1.gsfc.nasa.gov/new/validation-Report/Technology/TRW_EOI_Papers_Presentations/19.pdf
10. McCabe, G. H., Reuter, D. C., Dimitrov, R., Jennings, D. E., Matsumura, M. M., Rapchun, D. A. and Travis, J. W., The LEISA/atmospheric corrector (LAC) on EO-1. Geoscience and Remote Sensing Symposium, IGARSS '01. IEEE 2001 International, 2001, vol. 1, pp. 46–48; doi:10.1109/IGARSS.2001.976053.
11. Cutter, M. A., Compact high resolution imaging spectrometer (CHRIS) design and performance. In Proceeding of SPIE 5546, Imaging Spectrometry X, 126, 15 October 2014; doi:10.1117/12.560962.
12. Hoogeveen, R. W. M., Goede, A. P. H., Slijkhuis, S., Selig, A. and Burrows, J. P., Scanning imaging absorption spectrometer for atmospheric cartography (SCIAMACHY) development. *Proc. SPIE 2209*, Space Optics 1994; Earth Observation and Astronomy, 78, 13 September 1994; doi:10.1117/12.185288.
13. Zhao, X., Xiao, Z., Kang, Q., Li, Q. and Fang, L., Overview of the Fourier transform hyperspectral imager (HSI) boarded on the HJ-1 Satellite, 2010.
14. Lockwood, R. B. *et al.*, Advanced responsive tactically effective military imaging spectrometer (ARTEMIS): system overview and objectives. *Proc. SPIE 6661*, Imaging Spectrometry XII, 666102, 12 September 2007; doi: 10.1117/12.735844.
15. Kumar, A., Saha, A. and Dadhwal, V. K., Some issues related with sub-pixel classification using HYSI data from IMS-1 satellite. *J. Indian Soc. Remote Sensing*, 2010, **38**(2), 203–210; doi:10.1007/s12524-010-0027-5.
16. Kiran Kumar, A. S. *et al.*, The hyperspectral imager instrument on Chandrayaan-1. In 40th Lunar and Planetary Science Conference, The Woodlands, Texas, 23–27 March 2009.
17. Bisht, R. S. *et al.*, Limb viewing hyper spectral imager (LiVHySI) for airglow measurements onboard YOUTHSAT-1. *Adv. Space Res.*, 2014, **54**, 554–563; doi:10.1016/j.asr.2014.01.016.

ACKNOWLEDGEMENTS. We thank Shri A. S. Kiran Kumar, Director, SAC, ISRO, Ahmedabad for guidance and Shri D. R. M. Samudraiah and Shri P. N. Babu (SAC) for guidance and encouragement.